Title

Two-dimensional infrared spectroscopy reveals the complex behaviour of an amyloid fibril inhibitor.

Journal

Nature chemistry, 4(5)

ISSN

1755-4330

Authors

Middleton, Chris T
Marek, Peter
Cao, Ping
et al.

Publication Date

2012-03-01

DOI

10.1038/nchem.1293

Peer reviewed

HHS Public Access

Author manuscript

Nat Chem. Author manuscript; available in PMC 2012 November 01.

Published in final edited form as:

Nat Chem. ; 4(5): 355–360. doi:10.1038/nchem.1293.

Two-dimensional infrared spectroscopy reveals the complex behavior of an amyloid fibril inhibitor

Chris T. Middleton[a], **Peter Marek**[b], **Ping Cao**[b], **Chi-cheng Chiu**[c], **Sadanand Singh**[c], **Ann Marie Woys**[a], **Juan J. de Pablo**[c], **Daniel P. Raleigh**[b], and **Martin T. Zanni**[a,1]

[a]Department of Chemistry, University of Wisconsin-Madison, Madison, WI 53706-1396

[b]Department of Chemistry, State University of New York at Stony Brook, Stony Brook, NY 11794-3400

[c]Department of Chemical Engineering, University of Wisconsin-Madison, Madison, WI 53706-1396

Abstract

While amyloid formation has been implicated in the pathology of over twenty human diseases, the rational design of amyloid inhibitors is hampered by a lack of structural information about amyloid-inhibitor complexes. We use isotope labeling and two-dimensional infrared spectroscopy to obtain a residue-specific structure for the complex of human amylin, the peptide responsible for islet amyloid formation in type 2 diabetes, with a known inhibitor, rat amylin. Based on its sequence, rat amylin should block formation of the C-terminal β-sheet, but at 8 hours after mixing rat amylin blocks the N-terminal β-sheet instead. At 24 hours after mixing, rat amylin blocks neither β-sheet and forms its own β-sheet most likely on the outside of the human fibrils. This is striking because rat amylin is natively disordered and not previously known to form amyloid β-sheets. The results show that even seemingly intuitive inhibitors may function by unforeseen and complex structural processes.

INTRODUCTION

There is great interest in developing inhibitors of protein aggregation and amyloid formation as a means of combating Alzheimer's disease, Parkinson's disease, type 2 diabetes, and other human diseases[1–3]. Many types of inhibitors have been investigated, but the most common are small molecules[4,5] and peptides[6–13]. A common strategy for designing peptide

[1]To whom correspondence may be addressed: Martin T. Zanni, Department of Chemistry, University of Wisconsin-Madison, Madison, WI 53706-1396, 608 262-4783, zanni@chem.wisc.edu.

AUTHOR CONTRIBUTIONS

C.T.M., D.P.R. and M.T.Z. designed the research. C.T.M. performed the 2D IR and electron microscopy measurements. P.M., A.W.M. and P.C. synthesized and purified peptides. P.M and P.C performed the thioflavin-T fluorescence measurements. C.C., S.S and J.J.d.P designed and performed the molecular dynamics simulations. C.T.M. and M.T.Z. analyzed data. C.T.M., D.P.R. and M.T.Z. wrote the manuscript and coordinated contributions by other authors.

ADDITIONAL INFORMATION

The authors declare no competing financial interests. Supplementary information accompanies this paper at www.nature.com/naturechemistry. Reprints and permission information is available online at http://www.nature.com/reprints.

or peptide-mimic inhibitors involves two features[6,8,13]: (a) high sequence similarity with one region of the target protein to promote binding and (b) mutations in a second region so as to destabilize or prevent the formation of fibrils or oligomers. Mutations often include unnatural amino acids[6,7,9], or natural amino acids such as proline, that act as β-sheet blockers[11,12].

A range of peptide inhibitors have been developed against human amylin[8–12] (islet amyloid polypeptide or IAPP) the causative agent of islet amyloid in type 2 diabetes. While it is straightforward to test whether an inhibitor prevents fibril formation *in vitro*, without detailed structural information, it is very difficult to determine why some potential inhibitors are effective and others fail. For example, rat amylin has many of the features that one utilizes in inhibitor design including sequence similarity to human amylin and β-blocking proline residues (see Fig. 1a). It also does not form fibrils under any previously known conditions and rats do not get type 2 diabetes. Indeed, the rat amylin sequence has been used as the basis for designing an FDA-approved hypoglycemic agent for diabetics[14]. But in practice, rat amylin is only a moderately effective inhibitor; it must be present in ~10-fold excess to strongly inhibit human amylin fibril formation. With equimolar rat amylin (the ratio used in this study) 10–15% fewer fibrils are formed and the lag time for fibril formation is increased roughly two fold[12]. It is difficult to rationally improve the effectiveness of rat amylin because there is no structural information on the human amylin-inhibitor complex, at any point in the aggregation process, to guide design.

Rat amylin has been shown to inhibit amyloid formation by human amylin using thioflavin-T fluorescence, circular dichroism spectroscopy, and transmission electron microscopy (TEM)[12], which are methods that are widely employed in inhibitor studies. However, these techniques do not provide sufficient structural information to determine the binding. Mutagenesis, thermodynamics and other approaches can together provide considerable insight into inhibitor mechanisms[15–17]. Solid-state NMR[18,19] and molecular dynamics simulations[20] have been used to study inhibitor binding to some amyloid fibrils and X-ray structures of amyloids formed from short peptides have been used to design inhibitors[21]. These relatively few studies are a testament to the difficulty of obtaining atomic or even residue-level structural information on inhibitor binding.

Here we use isotope labeling and two-dimensional infrared (2D IR) spectroscopy to study the structure of an amylin-inhibitor complex with residue-level resolution. Structural models of human amylin fibrils reveal that they are made up of columns of U-shaped peptides (Fig. 1b) that form in-register parallel β-sheets. Each column has a C-terminal β-sheet (residues ~25 to 37) and an N-terminal β-sheet (residues 8 to ~17) that are separated by a partially ordered loop (residues ~18 and ~22)[22,23]. Between 2 and 5 columns of peptides form a fibril, depending on the preparation conditions[22,24]. A key feature of the structure is the in-register parallel β-sheet geometry, which is ideally suited for study by IR spectroscopy. If a backbone carbonyl is labeled with a $^{13}C^{18}O$ isotope, a linear column of vibrationally coupled residues is created in the fibril (Fig. 1c). The frequency of a linear column of coupled oscillators is shifted from the intrinsic vibrational frequency by twice the coupling strength[25,26]. We previously used these frequency shifts to study the residue-specific aggregation kinetics of amylin[27]. In this paper, we use the frequency shifts to determine the

binding site of the inhibitor. We also show that the inhibitor remodels the fibril into a structure not previously observed. The results are striking because rat amylin forms its own β-sheets, most likely on the exterior of the human amylin fibrils, in a dynamic process that is not evident from thioflavin-T fluorescence kinetics or from TEM measurements. The experiments reveal that inhibition, even for seemingly intuitively designed inhibitors, can be a complex process with details that require both structural and temporal resolution to uncover.

RESULTS AND DISCUSSION

Isotope Labeling Strategy

To assess the structure at each residue, we perform two control measurements without inhibitor. The control experiments account for site-to-site frequency variations caused by effects other than β-sheet formation, such as hydrogen bonding, environment electrostatics, and structural disorder. For each site, we first measure the spectrum of a sample in which only 25% of the peptides are labeled. At 25% dilution, only ~5% of labels form columns longer than three labels (see Supplemental). Thus, isotopic dilution eliminates the linear columns of labels so that the peak maximum provides the zero-coupling frequency for the site. We then measure the spectrum of a sample in which 100% of the peptides are labeled, providing the fully coupled frequency for the site. Two residues, Ala5 and Ser20, are in disordered regions of the fibril and did not exhibit a frequency difference (Supplementary Fig. S1). However, in most cases, the frequency difference between the pure-labeled and dilute-labeled samples gives the frequency shift caused by the coupling, which is directly related to structure[25].

Finally, we measure the spectrum of 100% labeled human amylin and unlabeled rat amylin, mixed as monomers at equimolar concentrations and matured together. Comparison of the mixed spectra with the two control spectra reveals the extent to which the inhibitor reduces the frequency shift. If the frequency shift remains appreciably negative or is unchanged, then the β-sheet is intact at this site. If the frequency shift is lost then the inhibitor has disrupted the β-sheet at this position. Therefore, isotope labeling provides a direct, site-specific, non-perturbing probe of the degree to which the inhibitor disrupts β-sheet structure in the amylin-inhibitor complex.

Structure of the Amyloid-Inhibitor Complex

Since thioflavin-T kinetics suggest that the amylin-inhibitor complex is equilibrated by 8 hours (Supplementary Fig. S2), we collected 2D IR spectra at 8 and 24 hours after mixing. At 8 hours, sets of 2D IR spectra were collected for 9 residues, chosen because they are spaced throughout the amylin sequence (Fig. 1b). Shown in Fig. 2 are spectra for residues Ala13, Leu16, Ala25 and Leu27. Ala13 has one of the largest frequency shifts, from 1598 cm^{-1} in the dilute-labeled spectrum (Fig. 2c) to 1580 cm^{-1} in the pure-labeled spectrum (Fig. 2a). This shift indicates that Ala13 resides in a highly ordered β-sheet[25,26], which is consistent with the solid-state NMR model of the fibril[22]. When mixed with the inhibitor, the Ala13 frequency shift is absent (Fig. 2b) indicating that Ala13 residues are now uncoupled. Similar observations are made by comparing the three spectra for Leu16 (Figs.

2d–f) and Ala8 (Supplementary Fig. S3). These results indicate that the N-terminal β-sheet structure is altered or eliminated by the inhibitor at these sites.

The inhibitor does not disrupt the coupling for all the measured residues. The spectra for two other labels, Ala25 and Leu27, are shown in Figs. 2g–l. For Leu27, there is a 20 cm^{-1} shift between the pure-labeled (Fig. 2l) and dilute-labeled (Fig. 2j) human amylin samples. The label frequency is still shifted by 12 cm^{-1} in the amylin-inhibitor complex. Thus, the coupling is diminished by 40% at Leu27, but is still very large. For Ala25, the frequency shift is unchanged in the presence of the inhibitor indicating that the inhibitor has not disrupted the ordered network of coupled sites. We also observed that coupling was retained for Val32 and Gly33 (Supplementary Fig. S3). These data show that the C-terminal β-sheet structure of the complex is highly similar to that of human fibrils.

Fig. 1b summarizes the results by plotting the outcome for each residue in relation to its position in the fibril structure. Residues for which the inhibitor eliminated the coupling are located in the N-terminal β-sheet of the amylin-inhibitor complex whereas residues for which the inhibitor had little or no effect lie in the C-terminal β-sheet. The results are summarized numerically in Table S1 and are reproducible (Supplementary Fig. S4–S7). The absence of excitonic coupling in the N-terminus suggests that rat amylin prevents formation of the exterior β-sheets in the amylinin-hibitor complex (Fig. 3a), but does not rule out the possibility that human-rat amylin β-sheets are formed (Fig. 3b). Mixed β-sheets seem likely since rat and human amylin have identical sequences in their first 17 residues and because fragments (residues 8–20) of both rat and human amylin are capable of forming fibrils on their own[28]. Thus either could contribute to forming the N-terminal β-sheet. However, 2D IR (Fig. 3c) and circular dichroism[12] spectra of the amylin-inhibitor complex compared with an equimolar mixture of rat amylin monomers and preformed human amylin fibrils, indicate that the complex contains less β-sheet and is more disordered than the canonical fibril.

To more precisely test whether the N-terminal of rat amylin replaces human amylin in the fibril structure, we isotope labeled Ala13 in both the rat and human peptides. 2D IR spectra are shown in (Figs. 3e–f). We find that the coupling at Ala13 is not restored in the complex when both rat amylin and human amylin are labeled. This lack of coupling eliminates the possibility of in-register mixed human-rat β-sheets, even though the N-terminal sequences of the two peptides are identical. Design principles would suggest that the similarity of the rat and human N-terminal sequences would promote binding to the N-terminal region while the prolines in rat amylin would prevent formation of the C-terminal β-sheet, but these structural studies show that rat amylin prevents the N-terminal β-sheet instead.

Long-term Structural Dynamics

All of the spectra reported above were collected 8 hours after mixing human amylin with the inhibitor. Eight hours was chosen because thioflavin-T fluorescence measurements indicate that the amylin-inhibitor complex has equilibrated by that time (Supplementary Fig. S2). However, 2D IR spectra collected 24 hours after mixing show that this is not the case. At 24 hours, the unlabeled β-sheet feature is more intense than at 8 hours (Fig. 3d) and significant excitonic coupling is detected between the Ala13-labeled human amylin peptides, which was absent at 8 hours (Fig. 2b vs. 3g), indicating that the N-terminal β-sheet is now formed.

One might assume that as the fibril fully forms, the inhibitor diffuses into solution and reverts back to its disordered monomeric structure, but that is not the case. At 24 hours, excitonic coupling is now present between Ala13-labeled rat amylin peptides (Fig. 3h). Therefore, rat amylin itself has also formed amyloidogenic parallel β-sheets. The formation of rat amylin β-sheets is unexpected because rat amylin does not form fibrils on its own (Supplementary Fig. S8, Ref. 12), or when added to preformed human amylin fibrils (Supplementary Fig. S9, Ref. 12) or in the presence of membrane bilayers[30–32]. We hypothesize that the exposed N-terminal region of human amylin in the amylin-inhibitor complex promotes the formation of rat amylin β-sheets by providing a template for the proper conformation and alignment of the rat amylin N-terminal region. Since the 2D IR data provides information on which residues form β-sheets, but not the number or stacking arrangement of the β-sheets in the fibrils, we also collected TEM images to probe fibril morphologies.

Human amylin fibrils prepared under our conditions produce long fibrils with a width of ~7 nm (Supplementary Fig. S10), which is consistent with previous studies using similar preparation protocols[22,24]. At 8 hours, TEM images of samples prepared with inhibitor show bundles of short fibrils with a large distribution of widths and a mode of ~13 nm (Fig. 4b and Supplementary Fig. S10). From our 2D IR data, we know that these structures have intact C-terminal β-sheets and denatured N-terminal β-sheets. We hypothesize that the denatured β-sheets promote the association of protofibrils into fibrils. At 24 hours, when both the human C- and N-terminal β-sheets are formed, the bundles are mostly replaced by long fibrils (Fig. 4c and Supplementary Fig. S10) with widths that approach those of pure human amylin fibrils (Fig. 4d and Supplementary Fig. S10). The rat amylin β-sheets may be forming on the exteriors of the human fibrils, since the fibril widths at 24 hours are slightly larger than for purely human fibrils at the same time, although other polymorphic structures cannot be ruled out nor can small structures that are not resolved by TEM. Nonetheless, the TEM images support the conclusion derived from the 2D IR studies that large structural changes occur between 8 to 24 hours even though thioflavin-T assays suggest that the system has equilibrated.

The model shown in Fig. 4e is consistent with our experimental data. Rat amylin interacts with human monomers or early stage oligomers, as indicated by a lengthening of the lag phase (Supplementary Fig. S2, Ref. 12). Mutation studies suggest that N-terminal residues are critical for these interactions[12]. Rat amylin initially inhibits the formation of the N-terminal β-sheets, but as time progresses, undergoes structural changes that allow the canonical human fibril structure to form. In doing so, the inhibitor peptides assemble into their own parallel β-sheets on the sides of the fibrils. Our illustration includes only one column of human peptides, but according to the TEM data, the bundles must consist of 2 or more columns of human amylin peptides. Since fully formed human amylin fibrils do not cause rat amylin to aggregate, it must be a transient complex that serves as a seed for rat amyloid β-sheet formation.

To explore the hypothesis that the amylin-inhibitor complex can promote the formation of rat amylin β-sheets, we used molecular dynamics simulations of one of the polymorphs derived from solid-state NMR data by Tycko et al.[22] The fibril consists of 10 amylin

peptides stacked into two columns of 5 peptides. This structure is stable for more than 100 ns. We modified the structure by pulling out residues 1–18 of the center amylin peptide, leaving a gap in the fibril, and inserted a rat amylin peptide in the simulation box such that it was bound to the displaced human peptide (Fig. 5a) in a parallel β-sheet conformation. Within 34 ns of starting the simulation, the human amylin β-strands translate to fill the gap caused by the missing N-terminus so that one β-sheet only has 4 strands while the other three have 5 strands. At no point in the simulation does the N-terminal strand reinsert itself. The inhibitor remains bound to the exposed human N-terminus and undergoes a structural change to form a partially ordered β-hairpin (Fig. 5b). This structure has not been observed in simulations of rat amylin monomers.[33] Even though we have only one trajectory and the ratio of rat to human amylin is much lower than in the experiments, it is interesting that the human fibril appears to be quite stable even with a mismatched number of N-terminal and C-terminal β-strands. It is also interesting that the N-terminal residues of both human and rat amylin remain in a stable β-sheet conformation that could serve to template further β-sheet formation. Further simulations will be highly beneficial for better understanding the interactions between human and rat amylin, not only by providing better statistics, but because 2D IR spectra can now be quantitatively calculated from molecular dynamics trajectories[29,34–36]. By helping quantify structural disorder, molecular dynamics simulations will enable us to extract more specific structural information from the data.

CONCLUSIONS

Our results illustrate the complexity involved in the *a priori* design of peptide inhibitors, particularly designs based on amino-acid sequence[6,7,9,10,37–39]). Both the recognition and β-blocking regions of rat amylin behave differently than expected, helping explain why rat amylin is only a moderate inhibitor of human amylin fibrils. The prolines residues do not prevent β-sheet formation by the human peptide, although they may slow the initial formation of β-structure. Indeed, the presence of three prolines ultimately prevents strong interactions with the C-terminal region, which could explain why rat amylin is a less-effective inhibitor than similar peptides with just a single proline residue[11,40]. We also find that the recognition sequence in rat amylin ultimately forms its own amyloidogenic β-sheets that could potentially increase toxicity. Therefore, peptide inhibitor design must also account for possibly detrimental amyloid-inhibitor complexes. Another key observation is that significant structural rearrangements still occur after the system has apparently equilibrated as judged by thioflavin-T experiments. Thioflavin-T fluorescence is possibly the most commonly used method for assessing amyloid β-sheet content. Our results indicate that Thioflavin-T measurements alone do not always accurately reflect the structural kinetics.

Our 2D IR method is general and can be applied to a wide range of inhibitors and as well as other aggregation-prone peptides, such as Aβ[26,41]. By providing structural insight into the amylin-inhibitor complex, 2D IR fosters rational drug design efforts for improving the efficacy of peptide and peptide-mimic amyloid inhibitors. It is also complimentary to solid-state NMR and X-ray studies of amyloid peptide fragments[21,42], because 2D IR spectroscopy, while it offers less detailed structural information, provides a rapid method to obtain critical residue-specific information. 2D IR can also provide mechanistic information through kinetic studies[27], which could be used to examine amyloid-inhibitor complexes

during the lag phase when oligomeric species are more prevalent. 2D IR spectroscopy can also be applied to membrane-bound systems[32,35,43–47], which accelerate amylin aggregation *in vitro*. In cases where human aggregation diseases are caused by proteins, native chemical ligation can be used to ^{13}C label segments or domains and the same strategy applied[48]. We also point out that the structural information reported here was all obtained using the diagonal peaks in the 2D IR spectrum. Thus, linear absorption spectra contain much of the same information. 2D IR spectroscopy has many benefits, such as the suppression of background absorbance, 2D lineshapes that give information about hydration[29,35,45], and cross peaks that probe secondary structures[25,49], but in principle the approach is available to any researcher with a standard FTIR spectrometer. Thus, both isotope-edited 1D and 2D IR spectroscopies can provide structural and mechanistic feedback to help understand and design amyloid inhibitors.

METHODS

Samples

All peptides were synthesized using solid-phase peptide synthesis and purified using HPLC, as previously described[50,51]. Amino acids labeled with ^{13}C,^{18}O isotopes were also prepared as previously reported[51,52]. Lyophilized peptides were dissolved to 1 mM concentration stock solutions in deuterated hexafluoroisopropanol. A portion of the stock solution was aliquoted, dried under nitrogen and then reconstituted in 5 μL of 20 mM phosphate D_2O buffer solution (pD ~7.4) to initiate aggregation. The final total peptide concentration for samples containing pure human amylin was 1 mM and for samples containing equimolar human and rat amylin was 2 mM. Samples were prepared in the same manner for all experiments.

2D IR Measurements

2D IR spectra were measured and processed using methods previously described[53]. Briefly, 60 fs (FHWM) mid-IR pulses were generated using a Ti:sapphire femtosecond laser system combined with an optical parametric amplifier. A mid-IR pulse shaping spectrometer[54,55] was used to collect the 2D IR spectra. Shot-to-shot phase cycling was performed to subtract scatter and collect data in the rotating frame. The probe signal was detected using a 64-element linear MCT array and digitized on a shot-by-shot basis. The polarization of the pump pulses were set perpendicular to the probe pulse. Samples prepared for 2D IR experiments were immediately transferred to a CaF_2 IR sample cell with a 56 μm Teflon spacer and kept under dry air to prevent hydrogen exchange from ambient water vapor.

Thioflavin-T Binding Kinetics

All fluorescence experiments were performed on an Applied Phototechnology fluorescence spectrophotometer using an excitation wavelength of 450 nm and an emission wavelength of 485 nm. The excitation and emission slits were 5 nm. The fluorescence intensity was measured once a second for the human amylin only kinetics and once a minute for the human and rat amylin mixture. The data is presented without any averaging. Samples were prepared by in the same manner and concentration as for 2D IR measurements except that

the buffer solution also contains 16 μM thioflavin-T. A 1.0 cm cuvette was used and the samples were not stirred, as in 2D IR measurements.

Transmission Electron Microscopy

TEM was performed at the University of Wisconsin Medical School Electron Microscope Facility. Samples were initially prepared in the same manner and concentration as for 2D IR measurements. Then, for each sample, a 2 μL aliquot was loaded onto a pioloform-coated copper grid and stained with methylamine tungstate (Nanoprobes, Inc.). Excess stain was blotted off, and the sample was allowed to air dry. Images were acquired by using a Philips CM 120 microscope with an accelerating voltage of 80 kV.

Full methods and any associated references are available in the online version of this Article.

Supplementary Material

Refer to Web version on PubMed Central for supplementary material.

ACKNOWLEDGMENTS

Support for this research was provided by the NIH grants DK79895 (M.T.Z), GM078114 (D.P.R.), and DK088184 (J.J.d.P) and the NSF through a CRC grant CHE 0832584 (M.T.Z and D.P.R.). We are grateful to Robert Tycko for providing the coordinates for his structural model of human amylin fibrils.

REFERENCES

1. Hardy J, Selkoe DJ. The amyloid hypothesis of Alzheimer's disease: Progress and problems on the road to therapeutics. Science. 2002; 297:353–356. [PubMed: 12130773]
2. Lorenzo A, Razzaboni B, Weir GC, Yankner BA. Pancreatic islet cell toxicity of amylin associated with type-2 diabetes mellitus. Nature. 1994; 368:756–760. [PubMed: 8152488]
3. Dawson TM, Dawson VL. Molecular pathways of neurodegeneration in Parkinson's disease. Science. 2003; 302:819–822. [PubMed: 14593166]
4. McLaurin J, et al. Cyclohexanehexol inhibitors of Aβ aggregation prevent and reverse Alzheimer phenotype in a mouse model. Nat. Med. 2006; 12:801–808. [PubMed: 16767098]
5. Roberts BE, Shorter J. Escaping amyloid fate. Nat. Struct. Mol. Biol. 2008; 15:544–546. [PubMed: 18523464]
6. Soto C, et al. β-sheet breaker peptides inhibit fibrillogenesis in a rat brain model of amyloidosis: Implications for Alzheimer's therapy. Nat. Med. 1998; 4:822–826. [PubMed: 9662374]
7. Gordon D, Tappe R, Meredith S. Design and characterization of a membrane permeable N-methyl amino acid-containing peptide that inhibits Aβ1–40 fibrillogenesis. J. Pep. Res. 2002; 60:37–55.
8. Kapurniotu A, Schmauder A, Tenidis K. Structure-based design and study of non-amyloidogenic, double N-methylated IAPP amyloid core sequences as inhibitors of IAPP amyloid formation and cytotoxicity. J. Mol. Biol. 2002; 315:339–350. [PubMed: 11786016]
9. Gilead S, Gazit E. Inhibition of amyloid fibril formation by peptide analogues modified with α-aminoisobutyric acid. Angew. Chem. Int. Ed. 2004; 43:4041–4044.
10. Yan L-M, Tatarek-Nossol M, Velkova A, Kazantzis A, Kapurniotu A. Design of a mimic of nonamyloidogenic and bioactive human islet amyloid polypeptide (IAPP) as nanomolar affinity inhibitor of IAPP cytotoxic fibrillogenesis. P. Natl. Acad. Sci. USA. 2006; 103:2046–2051.
11. Meng F, Raleigh DP, Abedini A. Combination of kinetically selected inhibitors in trans leads to highly effective inhibition of amyloid formation. J. Am. Chem. Soc. 2010; 132:14340–14342. [PubMed: 20873820]

12. Cao P, Meng F, Abedini A, Raleigh DP. The ability of rodent islet amyloid polypeptide to inhibit amyloid formation by human islet amyloid polypeptide has important implications for the mechanism of amyloid formation and the design of inhibitors. Biochemistry. 2010; 49:872–881. [PubMed: 20028124]
13. Zheng J, et al. Macrocyclic β-sheet peptides that inhibit the aggregation of a Tau-protein-derived hexapeptide. J. Am. Chem. Soc. 2011; 133:3144–3157. [PubMed: 21319744]
14. Hollander PA, et al. Pramlintide as an adjunct to insulin therapy improves long-term glycemic and weight control in patients With Type 2 diabetes. Diabetes Care. 2003; 26:784–790. [PubMed: 12610038]
15. Gazit E. Mechanisms of amyloid fibril self-assembly and inhibition. FEBS Journal. 2005; 272:5971–5978. [PubMed: 16302962]
16. Necula M, Kayed R, Milton S, Glabe CG. Small Molecule Inhibitors of Aggregation Indicate That Amyloid β Oligomerization and Fibrillization Pathways Are Independent and Distinct. J. Biol. Chem. 2007; 282:10311–10324. [PubMed: 17284452]
17. Porat Y, Abramowitz A, Gazit E. Inhibition of Amyloid Fibril Formation by Polyphenols: Structural Similarity and Aromatic Interactions as a Common Inhibition Mechanism. Chem. Biol. Drug Des. 2006; 67:27–37. [PubMed: 16492146]
18. Lamberto GR, et al. Structural and mechanistic basis behind the inhibitory interaction of PcTS on α-synuclein amyloid fibril formation. P. Natl. Acad. Sci. USA. 2009; 106:21057–21062.
19. Sato T, et al. Inhibitors of amyloid toxicity based on β-sheet packing of Aβ40 and Aβ42. Biochemistry. 2006; 45:5503–5516. [PubMed: 16634632]
20. Wu C, et al. The binding of thioflavin T and its neutral analog BTA-1 to protofibrils of the Alzheimer's disease Aβ16–22 peptide probed by molecular dynamics simulations. J. Mol. Biol. 2008; 384:718–729. [PubMed: 18851978]
21. Sievers SA, et al. Structure-based design of non-natural amino-acid inhibitors of amyloid fibril formation. Nature. 2011; 475:96–100. [PubMed: 21677644]
22. Luca S, Yau WM, Leapman R, Tycko R. Peptide conformation and supramolecular organization in amylin fibrils: constraints from solid-state NMR. Biochemistry. 2007; 46:13505–13522. [PubMed: 17979302]
23. Wiltzius JJW, et al. Atomic structure of the cross-β spine of islet amyloid polypeptide (amylin). Protein Sci. 2008; 17:1467–1474. [PubMed: 18556473]
24. Goldsbury CS, et al. Polymorphic Fibrillar Assembly of Human Amylin. J. Struct. Biology. 1997; 119:17–27.
25. Strasfeld DB, Ling YL, Gupta R, Raleigh DP, Zanni MT. Strategies for extracting structural information from 2D IR spectroscopy of amyloid: application to islet amyloid polypeptide. J. Phys. Chem. B. 2009; 113:15679–15691. [PubMed: 19883093]
26. Kim YS, Liu L, Axelsen PH, Hochstrasser RM. 2D IR provides evidence for mobile water molecules in β-amyloid fibrils. P. Natl. Acad. Sci. USA. 2009; 106:17751–17756.
27. Shim S-H, et al. Two-dimensional IR spectroscopy and isotope labeling defines the pathway of amyloid formation with residue-specific resolution. P. Natl. Acad. Sci. USA. 2009; 106:6614–6619.
28. Jaikaran ETAS, et al. Identification of a novel human islet amyloid polypeptide [beta]-sheet domain and factors influencing fibrillogenesis. J. Mol. Biol. 2001; 308:515–525. [PubMed: 11327784]
29. Wang L, et al. 2DIR spectroscopy of human amylin fibrils reveals robust β-sheet structure. 2011
30. Jayasinghe SA, Langen R. Lipid membranes modulate the structure of islet amyloid polypeptide. Biochemistry. 2005; 44:12113–12119. [PubMed: 16142909]
31. Knight JD, Hebda JA, Miranker AD. Conserved and cooperative assembly of membrane-bound α-helical states of islet amyloid polypeptide. Biochemistry. 2006; 45:9496–9508. [PubMed: 16878984]
32. Ling YL, Strasfeld DB, Shim S-H, Raleigh DP, Zanni MT. Two-dimensional infrared spectroscopy provides evidence of an intermediate in the membrane-catalyzed assembly of diabetic amyloid. J. Phys. Chem. B. 2009; 113:2498–2505. [PubMed: 19182939]

33. Reddy AS, et al. Solution Structures of Rat Amylin Peptide: Simulation, Theory, and Experiment. Biophys. J. 2010; 98:443–451. [PubMed: 20141758]
34. Falvo C, Hayashi T, Zhuang W, Mukamel S. Coherent Two Dimensional Infrared Spectroscopy of a Cyclic Decapeptide Antamanide. A Simulation Study of the Amide-I and A Bands. J. Phys. Chem. B. 2008; 112:12479–12490. [PubMed: 18781709]
35. Woys AM, et al. 2D IR line shapes probe ovispirin peptide conformation and depth in lipid bilayers. J. Am. Chem. Soc. 2010; 132:2832–2838. [PubMed: 20136132]
36. Smith AW, et al. Melting of a β-Hairpin Peptide Using Isotope-Edited 2D IR Spectroscopy and Simulations. J. Phys. Chem. B. 2010; 114:10913–10924. [PubMed: 20690697]
37. Poduslo JF, Curran GL, Kumar A, Frangione B, Soto C. β-sheet breaker peptide inhibitor of Alzheimer's amyloidogenesis with increased blood–brain barrier permeability and resistance to proteolytic degradation in plasma. J. Neurobiol. 1999; 39:371–382. [PubMed: 10363910]
38. Takahashi T, Mihara H. Peptide and protein mimetics inhibiting amyloid β-peptide aggregation. Acc. Chem. Res. 2008; 41:1309–1318. [PubMed: 18937396]
39. Sellin D, Yan L-M, Kapurniotu A, Winter R. Suppression of IAPP fibrillation at anionic lipid membranes via IAPP-derived amyloid inhibitors and insulin. Biophys. Chem. 2010; 150:73–79. [PubMed: 20153100]
40. Abedini A, Meng F, Raleigh DP. A single-point mutation converts the highly amyloidogenic human islet amyloid polypeptide into a potent fibrillization inhibitor. J. Am. Chem. Soc. 2007; 129:11300–11301. [PubMed: 17722920]
41. Kim YS, Liu L, Axelsen PH, Hochstrasser RM. Two-dimensional infrared spectra of isotopically diluted amyloid fibrils from Aβ40. P. Natl. Acad. Sci. USA. 2008; 105:7720–7725.
42. Bayro MJ, et al. Intermolecular structure determination of amyloid fibrils with magic-angle spinning and dynamic nuclear polarization NMR. J. Am. Chem. Soc. 2011; 133:13967–13974. [PubMed: 21774549]
43. Mukherjee P, Kass I, Arkin I, Zanni MT. Picosecond dynamics of a membrane protein revealed by 2D IR. P. Natl. Acad. Sci. USA. 2006; 103:3528–3533.
44. Fang C, Senes A, Cristian L, DeGrado WF, Hochstrasser RM. Amide vibrations are delocalized across the hydrophobic interface of a transmembrane helix dimer. P. Natl. Acad. Sci. USA. 2006; 103:16740–16745.
45. Manor J, et al. Gating mechanism of the influenza A M2 channel revealed by 1D and 2D IR spectroscopies. Structure. 2009; 17:247–254. [PubMed: 19217395]
46. Ghosh A, Qiu J, DeGrado WF, Hochstrasser RM. Tidal surge in the M2 proton channel, sensed by 2D IR spectroscopy. P. Natl. Acad. Sci. USA. 2011; 108:6115–6120.
47. Remorino A, Korendovych IV, Wu Y, DeGrado WF, Hochstrasser RM. Residue-specific vibrational echoes yield 3D structures of a transmembrane helix dimer. Science. 2011; 332:1206–1209. [PubMed: 21636774]
48. Moran SD, et al. Two-dimensional IR spectroscopy and segmental ^{13}C labeling reveals the domain structure of human γD-crystallin amyloid fibrils. P. Natl. Acad. Sci. USA. 2012
49. Maekawa H, De Poli M, Toniolo C, Ge N-H. Couplings between Peptide Linkages across a 310-Helical Hydrogen Bond Revealed by Two-Dimensional Infrared Spectroscopy. J. Am. Chem. Soc. 2009; 131:2042–2043. [PubMed: 19199613]
50. Abedini A, Raleigh DP. Incorporation of pseudoproline derivatives allows the facile synthesis of human IAPP, a highly amyloidogenic and aggregation-prone polypeptide. Org. Lett. 2005; 7:693–696. [PubMed: 15704927]
51. Marek P, Woys AM, Sutton K, Zanni MT, Raleigh DP. Efficient microwave-assisted synthesis of human islet amyloid polypeptide designed to facilitate the specific incorporation of labeled amino acids. Org. Lett. 2010; 12:4848–4851. [PubMed: 20931985]
52. Marecek J, et al. A simple and economical method for the production of ^{13}C,^{18}O-labeled Fmoc-amino acids with high levels of enrichment: applications to isotope-edited IR studies of proteins. Org. Lett. 2007; 9:4935–4937. [PubMed: 17958432]
53. Middleton CT, Woys AM, Mukherjee SS, Zanni MT. Residue-specific structural kinetics of proteins through the union of isotope labeling, mid-IR pulse shaping, and coherent 2D IR spectroscopy. Methods. 2010; 52:12–22. [PubMed: 20472067]

54. Shim S-H, Strasfeld DB, Zanni MT. Generation and characterization of phase and amplitude shaped femtosecond mid-IR pulses. Opt. Express. 2006; 14:13120–13130. [PubMed: 19532209]

55. Shim S-H, Zanni MT. How to turn your pump-probe instrument into a multidimensional spectrometer: 2D IR and Vis spectroscopies via pulse shaping. PCCP. 2009; 11:748–761. [PubMed: 19290321]

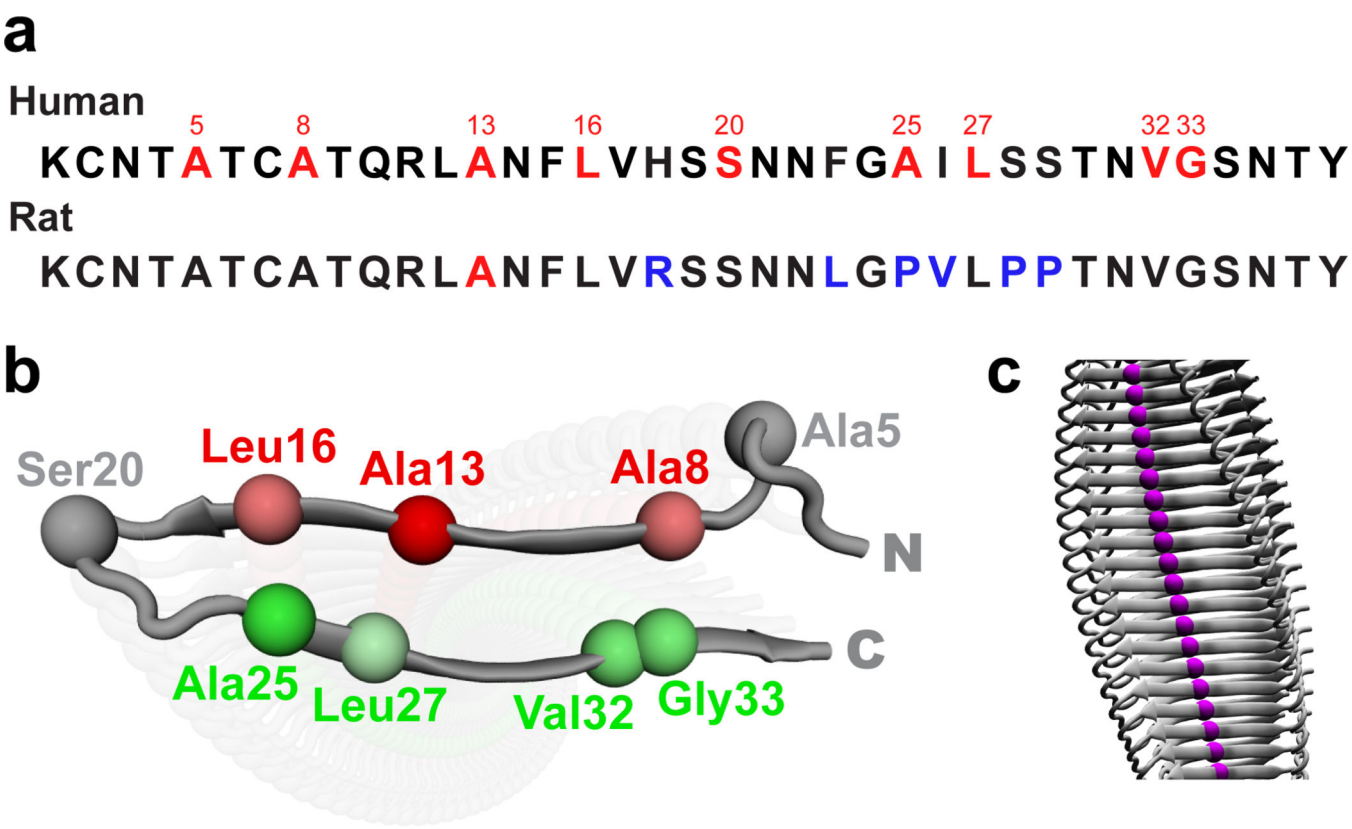

Figure 1. Sequence of human and rat amylin and structural model of human amylin fibrils

(**a**) Sequence of human and rat amylin, with $^{13}C^{18}O$ isotope labeled residues (red) and sequence differences (blue). (**b**) Depiction of a human amylin fibril viewed along the fibril axis with the sites of measured residues (spheres). The spheres are colored to summarize the labeled 2D IR spectra results shown in Figure 2b. Thus they show the effect of rat amylin on the inter-label coupling: bright red: ~100% loss of coupling, medium red: ~80% loss, light green: ~40% loss, medium green: ~35% loss, bright green: ~20% loss, grey: not measureable. (**c**) View of the fibril perpendicular to the fibril axis, with a label at a single residue shown (red spheres) in order to illustrate the formation of a linear chain.

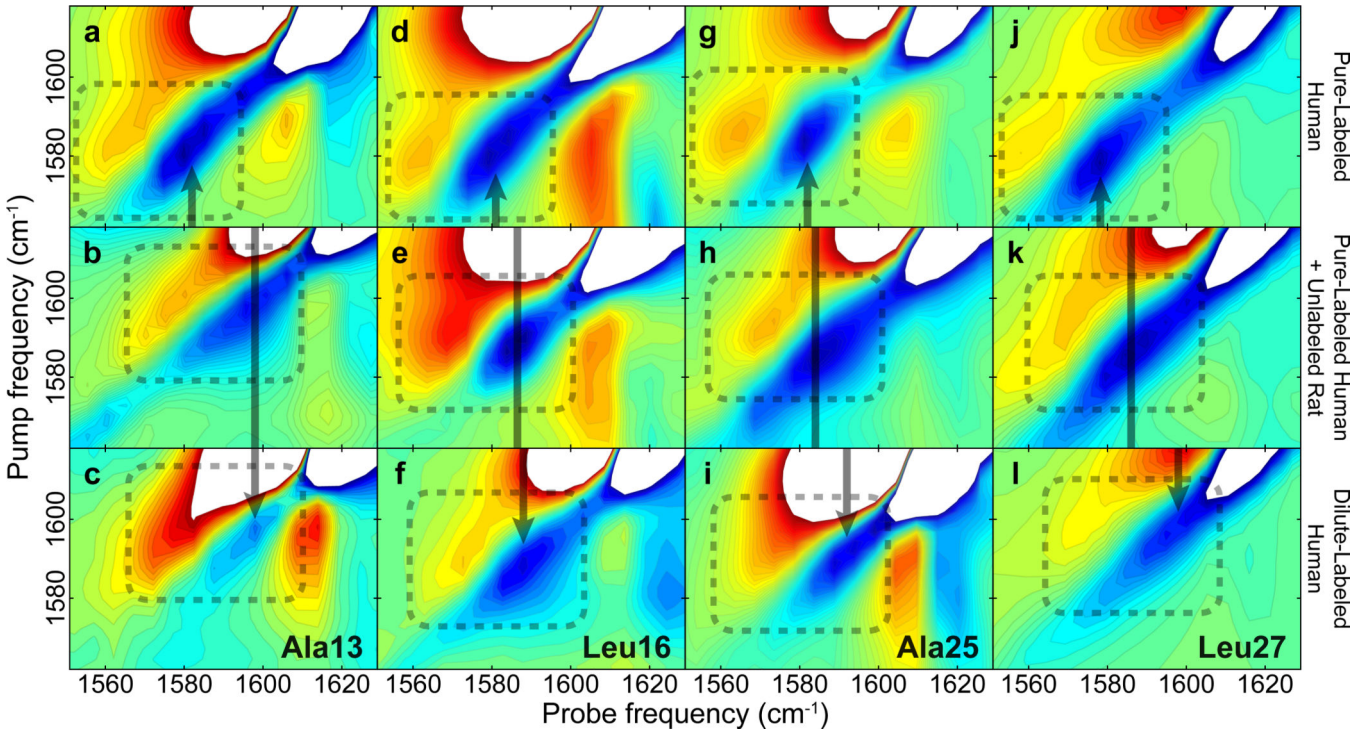

Figure 2. Rat amylin prevents human amylin from forming N-terminal, and not C-terminal, β-sheets at 8 hours after mixing

2D IR spectra of $^{13}C^{18}O$ labeled human amylin. Top row: pure-labeled human amylin fibrils. Middle row: equimolar mixture of human and rat amylin. Bottom row: dilute-labeled human amylin fibrils. Each column of panels shows spectra with human amylin labeled at different residues: Ala13 (**a–c**), Leu16 (**d–f**), Ala25 (**g–i**) and Leu27 (**j–l**). Label features are highlighted with dashed rectangles and the label frequencies are marked with black vertical lines to highlight the shifts. The Ala13 and Leu16 label frequencies in the human-rat mixture closely match their respective dilute-labeled frequencies, showing that the rat peptide disrupts the β-sheet coupling at these residues. On the other hand, the Ala25 and Leu27 label frequencies are closest to their respective pure-labeled frequencies, showing that the β-sheet structure at these residues is largely intact. See Supplementary Figs. S1 and S3 for spectra of residues Ala5, Ala8, Ser20, Val32 and Gly33.

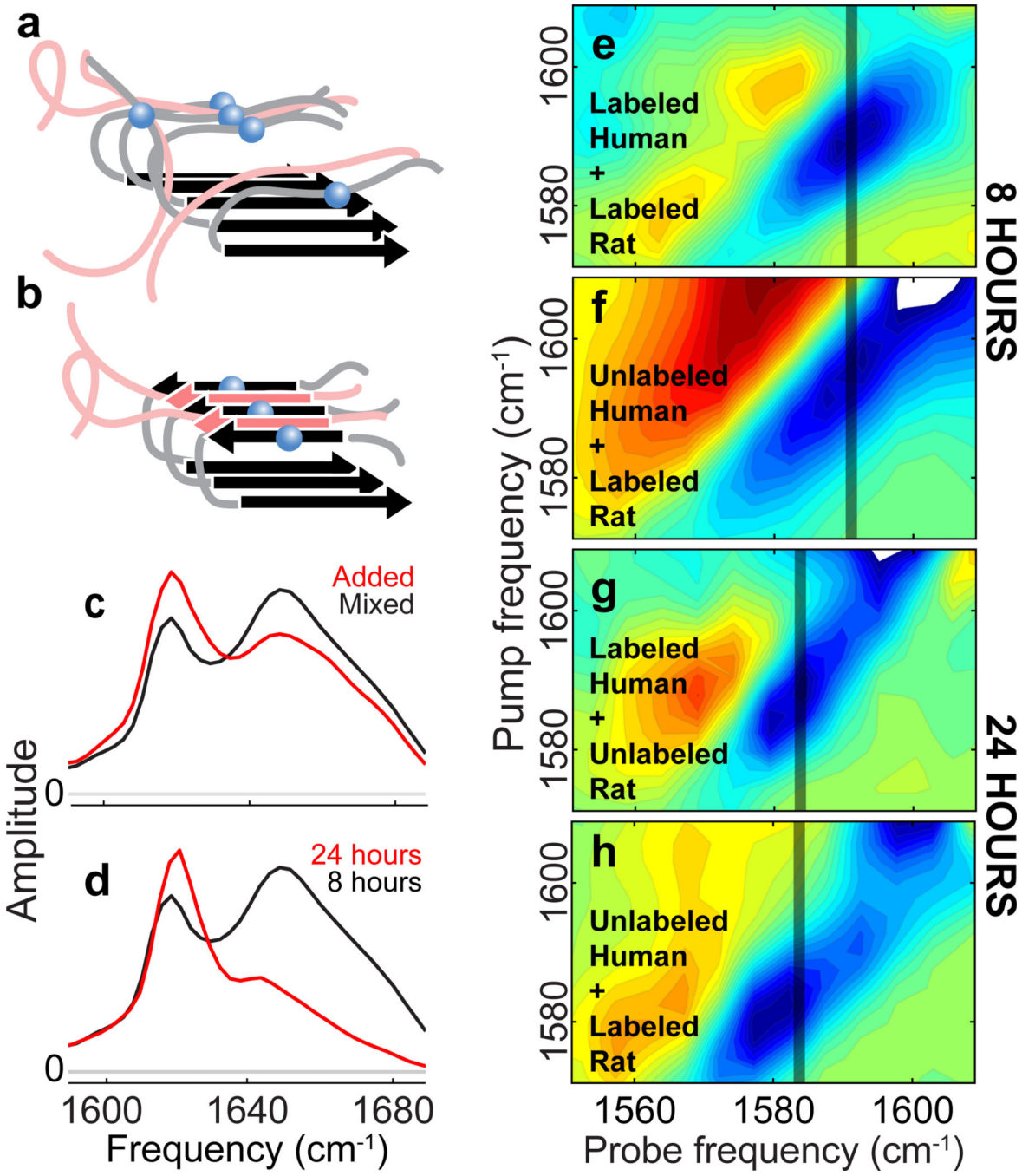

Figure 3. Human amylin β-sheets, initially disrupted by rat amylin, eventually form and promote the formation of rat amylin β-sheets

(**a**) and (**b**), Possible structures of amylin-inhibitor complex. Ala13 isotope labels are shown as blue spheres. (**a**) Rat amylin (pink) prevents formation of the N-terminal β-sheet by human amylin (grey). (**b**) Rat and human amylin form mixed β-sheets. (**c**) Diagonal slices of unlabeled human and rat amylin mixtures. Rat amylin monomers added to preformed human amylin fibrils (red). (**d**) Diagonal slices through the unlabeled region of equimolar mixtures of human and rat amylin after 8 hours (black) and 24 hours (red). (**e**) 2D IR spectrum of

amylin-inhibitor complex with both human and rat amylin labeled at Ala13. (**f**) 2D IR spectrum of amylin-inhibitor complex with unlabeled human amylin and Ala13-labeled rat amylin. Rat and human amylin mixed as monomers and matured together (black). (**g**) 2D IR spectrum of Ala13-labeled human amylin after 24 hours in the presence of unlabeled rat amylin. (**h**) 2D IR spectrum of Ala13-labeled rat amylin after 24 hours in the presence of unlabeled human amylin. For **e, f, g** and **h**, the Ala13 feature was isolated by subtracting the corresponding unlabeled spectrum (see Supplemental for details).

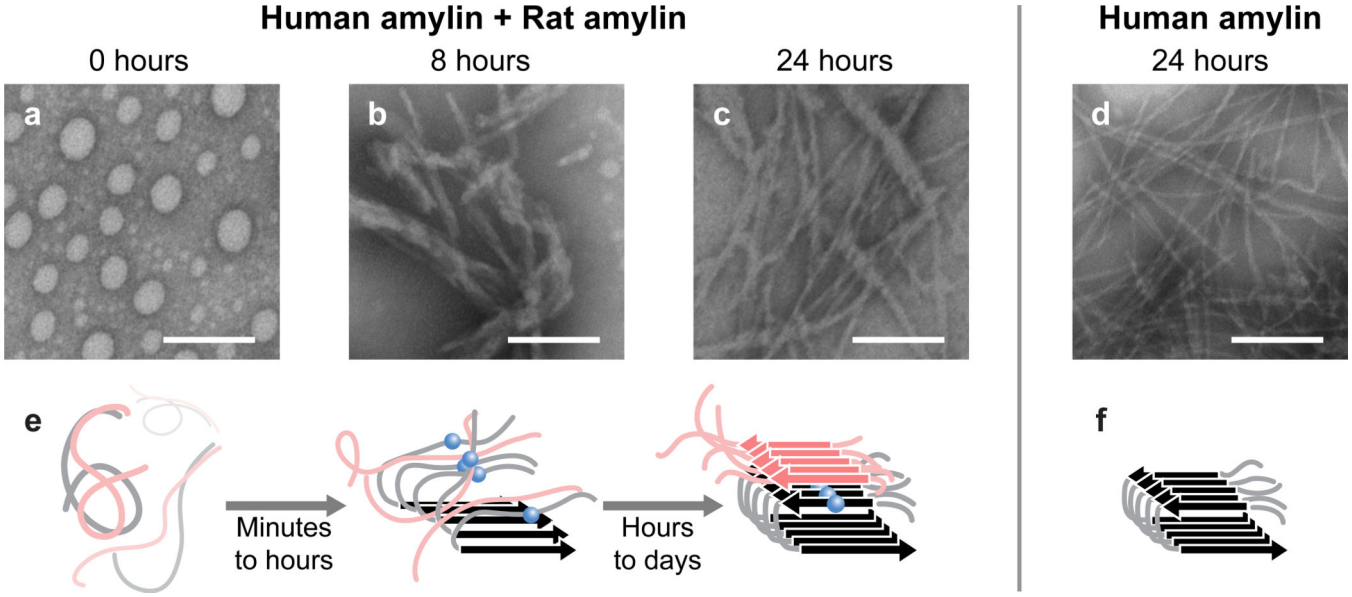

Figure 4. Electron microscopy supports the unexpected structural dynamics revealed by 2D IR results

TEM images of human and rat amylin mixture (**a**) after initial mixing, (**b**) at 8 hours, and (**c**) at 24 hours. (**d**) TEM image of human amylin at 24 hours. (**a–d**) Scale bars represent 100 nm. Short, disordered structures are observed for the human-rat mixture at 8 hours while longer, fibril structures are observed at 24 hours. The fibrils observed in the human-rat mixture are thicker than human-only fibrils, suggesting the mechanism shown in panel **e**. (**e**) Rat (pink) and human (grey) peptides interact as monomers or early-stage oligomers. At 8 hours, rat amylin prevents β-sheet formation for the region of human amylin containing residues Ala8, Ala13 and Leu16. At 24 hours, human amylin forms the N-terminal β-sheet and rat amylin forms ordered β-sheet structures templated by the human fibrils. Human Ala13 isotope labels are shown as blue spheres. (**f**) Schematic diagram of a human amylin fibril.

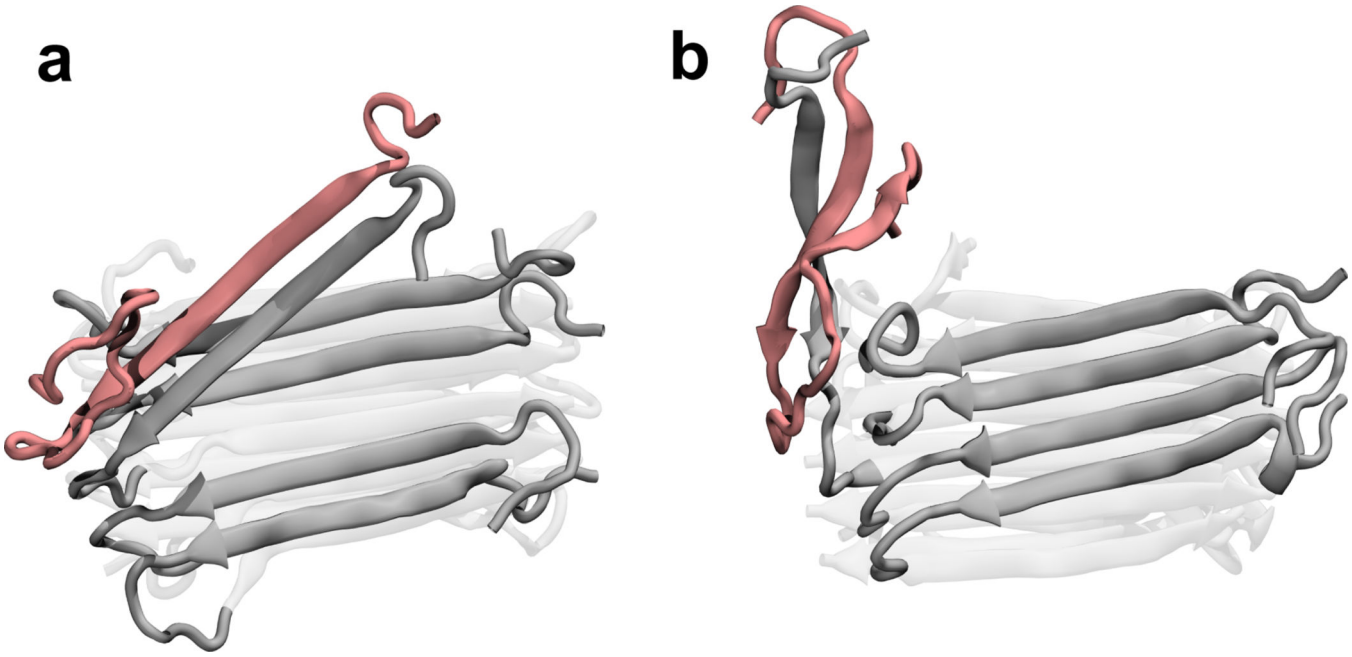

Figure 5. Molecular dynamics simulation suggests that the N-terminals of human and rat amylin can form a partially ordered β-sheet complex

Human (grey) and rat (pink) amylin form a stable complex in which the N-terminal residues of both peptides are in a β-sheet conformation, which could promote formation of the rat amylin β-sheets detected in the 2D IR measurements. The N-terminal β-sheet of the fibril can close to heal the gap left by the extracted human N-terminus. (**a**) The starting configuration of simulation. (**b**) The configuration after 75 ns. The back half of the fibril model is lightened to clarify the structural changes in the front half.